Biomaterials 31 (2010) 7985–7994

Contents lists available at ScienceDirect

Biomaterials

journal homepage: www.elsevier.com/locate/biomaterials

FGF-2 and VEGF functionalization of starPEG–heparin hydrogels to modulate biomolecular and physical cues of angiogenesis

Andrea Zieris, Silvana Prokoph, Kandice R. Levental, Petra B. Welzel, Milauscha Grimmer, Uwe Freudenberg, Carsten Werner*

Leibniz Institute of Polymer Research Dresden (IPF), Max Bergmann Center of Biomaterials Dresden (MBC) & Technische Universität Dresden (TUD), Center for Regenerative Therapies Dresden (CRTD), Hohe Str. 6, 01069 Dresden, Germany

ARTICLE INFO

Article history:
Received 27 May 2010
Accepted 4 July 2010
Available online 3 August 2010

Keywords:
Biohybrid hydrogel
Fibroblast growth factor 2
Vascular endothelial growth factor
Growth factor release system
Angiogenesis

ABSTRACT

Tissue engineering therapies require biomaterials capable of encouraging an angiogenic response. To dissect the influence of different pro-angiogenic stimuli a set of starPEG–heparin hydrogels with varied physicochemical properties was used as a highly efficient reservoir and tunable delivery system for basic fibroblast growth factor (FGF-2) and vascular endothelial growth factor (VEGF). The engineered gel materials could be precisely tailored by decoupling the biomolecular functionalization from the variation of the viscoelastic matrix characteristics. Culture experiments with human umbilical vein endothelial cells (HUVECs) revealed the interplay of growth factor presentation, adhesive characteristics and elasticity of the gel matrices in triggering differential cellular behavior which allowed identifying effective pro-angiogenic conditions.

1. Introduction

Lack of vascularization is still a major issue for successful tissue engineering therapies. One approach to overcome this problem is to create biomaterials that are able to induce a localized angiogenic response by supporting the sprouting of new blood capillaries from pre-existing microvascular vessels after implantation at the target site [1,2]. For this purpose, corresponding strategies aim to create materials that are bioresponsive (to cell-associated external signals such as extracellular proteases and endoglycosidases), bioactive (by virtue of bound peptide or recombinant protein adhesion ligands and cytokines), as well as applicable into tissues in a minimally invasive manner [3,4]. Since biological processes such as angiogenesis are known to be influenced by both the physicochemical structure of the surrounding matrix as well as by biomolecular cues [5], many of these approaches are related to an imitation of the viscoelastic properties, bio-adhesive nature and proteolytic susceptibility of the extracellular matrix (ECM) [4]. However, none of the currently applied biomaterials allow for the systematic and independent variation of mechanical and biomolecular characteristics [6]. In particular, biomaterials to encourage angiogenesis need to mimick the ability of the ECM to bind and stabilize growth factors (GFs) and to control their localized presentation and release [7,8]. Although a variety of GFs are known to be involved in the regulation of this process [1], basic fibroblast growth factor (FGF-2) and vascular endothelial growth factor (VEGF) are among the most important ones, as both proteins are able to stimulate the proliferation, survival, motility and differentiation of endothelial cells [9–11]. Consequently, FGF-2 and VEGF are key mediators of new blood vessel growth in ischemia and wound healing which makes them particularly interesting for their use in therapeutic angiogenesis [12]. However, upon direct administration to the body, soluble GFs typically have a short half-life due to their rapid degradation after diffusion from the target site, which makes it necessary to stabilize them during their supply [13]. In vivo, both FGF-2 and VEGF can be stored by the ECM through interactions with sulfated glycosaminoglycans closely resembling the highly anionic polyelectrolyte heparin [14,15]. Here, binding mainly occurs via spatially matching electrostatic interactions between negatively charged N- and O-sulfated groups of heparin and the basic lysine and arginine residues of FGF-2 or VEGF [16,17]. Through binding to heparin, diffusion of GFs is decelerated [8]. The interaction with heparin leads to a protection against loss of their bioactivity (e.g. through proteolysis, [18,19]) while simultaneously potentiating receptor affinity [20,15]. Taking advantage of this effect, numerous recent advances focus on the design of heparin-containing biomaterials [21–25]. Moreover, by combining these systems with synthetic building blocks [26], hybrid materials can be created offering both a defined functionality and biocompatibility as well

* Corresponding author. Fax: +49 351 4658 533.
E-mail address: werner@ipfdd.de (C. Werner).

0142-9612/$ – see front matter © 2010 Elsevier Ltd. All rights reserved.
doi:10.1016/j.biomaterials.2010.07.021

as a high adaptability in terms of composition and structure. In the production of such hybrid systems, poly(ethylene-glycol) is one of the most commonly used synthetic components [27–31] since it provides excellent biocompatibility, a hydrophilic and uncharged character, and the possibility to easily modify its terminal end groups [32].

Recently, a biohybrid hydrogel formed by the crosslinking of amine functionalized star-shaped poly(ethylene-glycol) (starPEG) and carbodiimide/*N*-hydroxysulfosuccinimide (EDC/s-NHS)-activated heparin has been developed (Scheme 1, [33]). The gel materials utilize heparin as a multifunctional crosslinker to form tunable hydrogels and as compared to the formerly mentioned systems [27–31], are characterized by a significantly higher heparin concentration (up to 0.8% (w/w)) in the swollen matrices [33]. Since the structural integrity of heparin can therefore be preserved to higher degrees of crosslinking, this attribute permits rather unaffected interactions with heparin-binding GFs. As a second advantage, the biohybrid hydrogel system can be gradually and separately tuned in its structural characteristics and biomolecular functionalization [33]. Since angiogenesis is controlled by both molecular signals and the viscoelastic properties of the surrounding matrix [5], this approach offers a way to independently explore the influence of these factors on cellular behavior (Scheme 1).

In this study, the potential of starPEG–heparin hydrogels differing in their network characteristics to bind and release FGF-2 and VEGF has been evaluated. Moreover, the impact of the biofunctionalization together with the physicochemical properties of the scaffolds on the behavior of human umbilical vein endothelial cells (HUVECs) was analyzed.

2. Materials and methods

2.1. Preparation of starPEG–heparin hydrogel networks

StarPEG–heparin hydrogels were formed by crosslinking amino end-functionalized four-arm starPEG with EDC/s-NHS activated carboxylic acid groups of heparin [33]. For this, a total polymer content of 11.6% and a 2:1:1 ratio of EDC:s-NHS:NH_2-groups of starPEG [mol/mol] were used. The molar ratio of starPEG to heparin was varied from 1.5 to 6.

Heparin (14,000 g/mol; Calbiochem (Merck), Darmstadt, Germany) and starPEG (10,000 g/mol Polymer Source, Inc., Dorval, Canada) were each dissolved in one third of the total volume of ice-cold deionised, decarbonised water (MilliQ) by ultrasonication and afterwards kept on ice (approx. 2–4 °C). Similarly, EDC (Sigma–Aldrich, Munich, Germany) and s-NHS (Fluka, Seelze, Germany) were separately dissolved in the sixth part of the total volume of ice-cold MilliQ. Subsequently, EDC and s-NHS solutions were added to heparin, mixed well and incubated for 15 min on ice to activate heparin carboxylic groups. After that, the starPEG solution was added to the activated heparin and mixed for 15 min at 8 °C (at 900 rpm, Thermomixer Comfort, Eppendorf, Hamburg, Germany).

To allow for a practical performance of quantitative FGF-2 or VEGF binding/release studies and for cell culture experiments, surface-bound gels with a final thickness of approx. 50 μm were prepared. For this 3.11 μl of the gel mixture per cm^2 were used. All results presented are expressed for a scaffold prepared from 5.5 μl of the gel mixture. To obtain surface immobilized networks, the gel solution was placed on freshly aminofunctionalized glass cover slips or directly into aminofunctionalized glass bottom 24-well plates (Greiner Bio-One GmbH, Frickenhausen, Germany) to allow covalent attachment of heparin through its activated carboxylic acid groups [34]. In order to spread the solution equally, the mixture on the glass slides was covered with a hydrophobic glass cover slip that has been treated with hexamethyldisilazane (Fluka) from vapor phase or by placing an ethylen-chlortrifluorethylen-copolymer slide (Goodfellow, Cambridge, England) onto the gel solution in the glass bottom wells. For preparation of free-floating gel disks, 104.7 μl of the liquid gel mixture were placed onto a 1 cm^2 hydrophobic glass cover slip and covered with a second hydrophobic one.

After polymerization over night at 22 °C, the cover slips were removed. Gels were washed in phosphate buffered saline (PBS, Sigma–Aldrich) to remove EDC/s-NHS and any non-bound starPEG/heparin. PBS was exchanged five times, once per hour, and once again after storage for 24 h. Subsequently, the swollen gels were immediately used for further experiments. For cell culture, sterilization was performed by UV-treatment for 30 min. For additional treatments, all solutions were sterile unless otherwise indicated.

2.2. Biomodification of starPEG–heparin hydrogels

For biomodification with cyclo(Arg-Gly-Asp-D-Tyr-Lys) (Peptides International, Louisville, KY, USA) surface-bound swollen hydrogels were washed with 1/15 M phosphate buffer (pH 5) at 4 °C 3 times. Next, this solution was exchanged for EDC/s-NHS solution (50 mM EDC, 25 mM s-NHSin 1/15 M phosphate buffer (pH 5)) to activate the carboxylic acid groups of heparin. After incubation for 45 min the scaffolds were washed 3 times in borate buffer (100 mM, pH 8; 4 °C) to remove unbound ECD/s-NHS. Subsequently, the gels were incubated in 300 μl RGD-solution (50 μg/ml; dissolved in borate buffer) for 2 h at room temperature. Finally, all samples were washed in PBS 3 times.

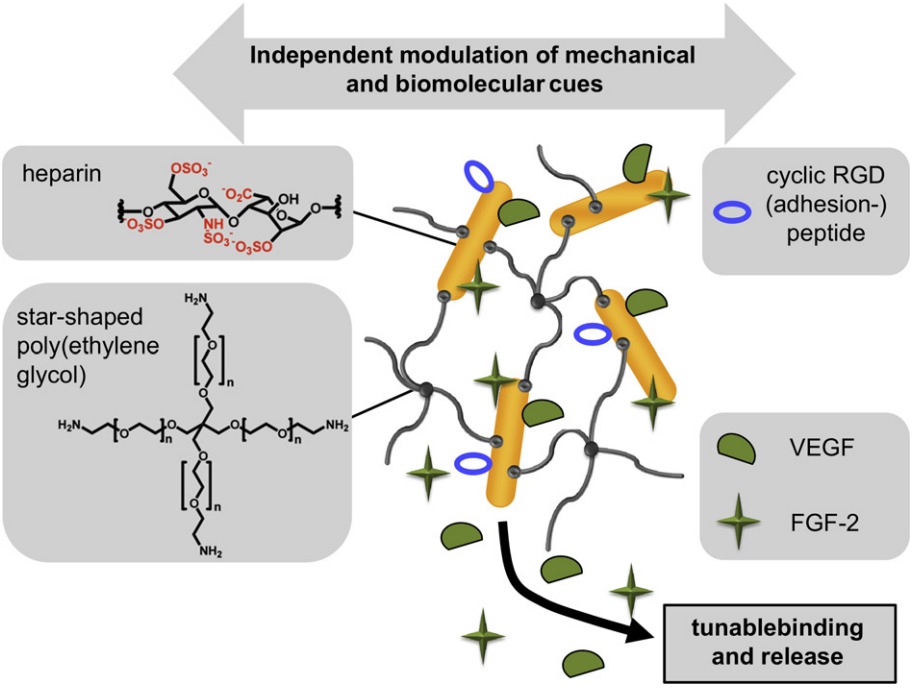

Scheme 1. Design of the starPEG–heparin hydrogels, showing decoupled mechanical and modular biomolecular characteristics.

To immobilize FGF-2 (Miltenyi Biotech, Bergisch Gladbach, Germany) or VEGF165 (PeproTech GmbH, Hamburg, Germany) to the starPEG–heparin networks, the particular protein was dissolved in PBS at the desired concentration (1 μg/ml unless otherwise indicated). PBS-swollen pure or RGD modified gels were immersed in 200 μl/cm^2 FGF-2 or VEGF solution at room temperature for 24 h followed by rinsing with PBS twice.

2.3. Analysis of starPEG–heparin hydrogel properties

StarPEG–heparin hydrogels were characterized as described elsewhere [33]. Briefly, the storage modulus of the final networks ($n = 4$) was determined using oscillating measurements on a rotational rheometer with plate-plate geometry (plate diameter 25 mm, gap width 1.2–1.5 mm). Dynamic frequency sweep tests under strain control were carried out at 25 °C in a shear frequency range of 10 + 2–10 − 1 rad/s. The strain amplitude was set to 3% and storage and loss modulus were measured as a function of the shear frequency. From this, pore sizes of the network could be estimated according to the rubber-elasticity theory as described in [33]. Volumetric swelling degree v_t was calculated by $v_t = (d_t/d_0)^3$, where d_0 is the diameter of a non-swollen gel disk and d_t is the diameter of the disk after the washing process in PBS for 24 h. The heparin and RGD content is expressed in relation to the final volume of the PBS-swollen gel network.

2.4. Characterization of the biomodification

2.4.1. confocal Laser Scanning Microscopy (cLSM)

FGF-2 or VEGF were labeled with tetramethylrhodamine (TAMRA) according to the FluoReporter Tetramethylrhodamine Protein Labeling Kit manual (Molecular Probes, distributed by Invitrogen, Netherlands). TAMRA-FGF-2 or VEGF were dissolved in PBS (5 μg/ml) and added to starPEG–heparin gels ($n = 2$, 200 μl/cm^2) that were directly immobilized in glass bottom 24-well plates. Fluorescence intensity was quantified using a Leica SP5 (Leica, Bensheim, Germany) confocal laser scanning microscope with a 40× magnification immersion objective (HCxPL APO, Leica) and aperture pinhole set at 68 μm. The argon-laser (excitation wavelength 488 nm, laser intensity 20%) was used for exciting Alexa 488-labeled gels whereas the DPSS laser (excitation wavelength of 561 nm, intensity 20%) was used for excitation of TAMRA-labeled FGF-2 or VEGF. Alexa 488 and TAMRA emission were analyzed in the 500–550 nm or 570–630 nm range, respectively.

The time-dependent intensity of the TAMRA-FGF-2 or VEGF was quantified for the solution (supernatant of the gel body) and for the gel body performing an XZ scan at defined intervals. Intensity profiles (XZ-scan) at three different X-positions were evaluated for each time point.

2.4.2. Enzyme-linked immunosorbent assay (ELISA)

Surface-bound gels ($n = 3$) were placed in custom-made incubation chambers that allowed only minimal interaction of the protein solution with areas not originating from the hydrogel. 200 μl of FGF-2 (0.5, 1, 5 or 50 μg/ml) or VEGF (0.5, 1, 5, 10 or 25 μg/ml) solution were added per cm^2. Immobilization was performed over night at 22 °C. The FGF-2 or VEGF solution was taken out followed by washing with PBS twice. Each of these solutions was collected and assayed in duplicates using an ELISA Quantikine kit (R&D Systems, Minneapolis, USA). After immobilization, FGF-2 or VEGF were allowed to release from these gels at 22 °C into 250 μl/cm^2 of serum-free (SF) endothelial cell growth medium (ECGM; Promocell GmbH, Heidelberg, Germany) supplemented with 0.02% sodium azide (Fluka). Samples taken at intervals were stored at −80 °C until analyzed by ELISA. An equal volume of fresh medium was added back at each time point.

2.4.3. Amino acid analysis via high performance liquid chromatography (HPLC)

Quantification of RGD-peptide (50 μg/ml; $n = 4$), FGF-2 (10, 25 or 50 μg/ml; $n = 2$), or VEGF (10, 25 or 50 μg/ml; $n = 2$) in the gels was performed by acidic hydrolysis and subsequent high performance liquid chromatography (HPLC) analysis as described elsewhere [35]. Briefly, gel-coated substrates or volume samples were subjected to vapor hydrolysis in vacuo using 6 M HCl at 110 °C for 24 h and subsequently neutralized. Extraction of amino acids from the samples was accomplished by repeated rinsing with a definite volume of 50 mM sodium acetate buffer at pH 6.8. The released amino acids were chromatographically separated after pre-column derivatization with ortho-phthalaldehyde on a Zorbax SBC18 column (4.6 × 150 mm, 3.5 μm, Agilent Technologies, Boeblingen, Germany) using an Agilent 1100 LC system (Agilent) with fluorescence detection. Amino acids were quantified using external standards.

2.4.4. Radiolabeling studies

^{125}I-labeled FGF-2 was purchased from Chelatec SAS (Nantes, France), VEGF was labeled with ^{125}I using IodoBeads (Pierce, Rockford, USA). For this, 1 mCi Na^{125}I (PerkinElmer Massachusetts, USA) dissolved in 100 μl of PBS (pH 7.4) was added to a single IodoBead that had been rinsed with PBS. After 5 min of incubation at room temperature, 200 μl VEGF stock (1 mg/ml) was added and allowed to react for 20 min. By size exclusion chromatography (NAP-5 column, GE Healthcare, Munich, Germany) using PBS as the eluent, unbound iodide was removed yielding iodinated protein with less than 2% free ^{125}I. The resulting protein concentration was determined by a UV/vis spectrometer (Eppendorf) while the specific activity of the protein solution was analyzed via gamma counting (LB 123, Berthold Technologies GmbH & Co. KG, Bad Wildbad, Germany).

To perform protein binding and release studies, surface-bound gels ($n = 2$–4) were placed in custom-made incubation chambers that decreased the exposure of the protein to surfaces not originating from the hydrogels to a minimum. Native FGF-2 or VEGF protein solution was spiked with ^{125}I-labeled FGF-2 or VEGF as a percentage of total protein (2.5–100%). This mixture containing 0.5, 1, 5 or 10 μg/ml FGF-2 or VEGF in PBS, respectively, was added to surface-bound hydrogels (200 μl per cm^2) and the protein was adsorbed over night at 22 °C. After the incubation period, gels were rinsed two times with an excess volume of PBS. Radioactivity was measured twice per sample using gamma counting. Immobilized protein was quantified using ^{125}I-FGF-2 or VEGF standards.

After immobilization, FGF-2 or VEGF were allowed to release from these gels ($n = 2$) at 22 °C into 250 μl/cm^2 of SF ECGM supplemented with 0.02% sodium azide. At defined time intervals, the medium was withdrawn and the remaining FGF-2 or VEGF bound to the gels was monitored twice via gamma counting. An equal volume of fresh medium was added back after each measurement.

2.5. Cell culture experiments

2.5.1. Cultivation of HUVECs

Human endothelial cells from the umbilical cord vein (HUVECs) were collected according to the procedure suggested by [36] and grown to confluence in SF ECGM. After one to four passages, 20,000 cells per 1.77 cm^2 surface were seeded on either pure starPEG–heparin networks or on scaffolds modified with FGF-2, RGD, or RGD/FGF-2 which were pre-equilibrated with SF ECGM for 30 min at 37 °C. Similarly, cells were grown on control surfaces consisting of immobilized fibronectin (FN) with or without 1 ng/ml FGF-2 or VEGF supplemented to the SF ECGM. For this, FN was isolated and purified from adult human plasma according to [37] and immobilized for 2 h to the bottom of 24-well plates (50 μg/ml dissolved in PBS; 450 μl per well). After rinsing these surfaces twice with PBS, cells could be seeded. On each material, cells were cultured for 3 days at 37 °C and 5% CO_2.

2.5.2. Survival studies

Analysis of cell survival was performed by Live/Dead staining as described by [38] after 3 days of culture on the different substrates ($n = 2$–4). For this, 2 ml of a solution containing 0.1 μg/ml fluorescein di-O-acetate (FDA; Fluka) and 2 μg/ml propidium iodide (PI; Fluka) dissolved in PBS were added to each sample and incubated for 2 min at 22 °C. The cells were then immediately visualized by fluorescence microscopy (DMIRE2, Leica) using a 10× dry objective (HC PL Fluotar 10 × 0.30, Leica). Thereby FDA fluorescence was monitored by excitation with an argon-laser (excitation wavelength 492 nm, emission wavelength 520 nm) whereas PI positive samples were excited with a helium-neon-laser (excitation wavelength 537 nm, emission wavelength 566 nm). Both images were combined to generate an overlay picture.

2.5.3. Proliferation assay

Cell proliferation was studied after 3 days of culture with the help of a 3-(4,5-dimethyl thiazol-2-yl)-2,5-diphenyltetrazoliumbromide (MTT; Sigma–Aldrich) proliferation assay as described by [39]. For this, 500 μl of a 1/5 mixture of MTT (5 mg/ml) and SF ECGM were added to each sample and incubated for 5 h at 37 °C. Next, the supernatant was removed completely from the substrates and 300 μl dimethyl sulfoxide (DMSO; Fluka, Seelze, Germany) was added. The samples were incubated for 20 min at 37 °C and afterwards 200 μl of the solution were transferred into a 96-well plate. Absorption was subsequently measured in a plate reader (Genios, TECAN, Crailsheim, Germany) at 540 nm. Experiments were performed for at least three samples.

2.5.4. Analysis of cell morphology

After 3 days of culture, light microscopy images were taken (Olympus IX50, Olympus, Hamburg, Germany) with 10× magnification. Resulting cell morphology in dependence on the culture conditions was analyzed using the circularity calculation within ImageJ 1.41° (developed by W. Rasband, National Institutes of Health, Bethesda, USA) by tracing cell boundaries manually. Here, a circularity of '1' corresponds to a fully circular object, while a value of '0' represents a straight line. For each condition, between ~30 and 200 cells were analyzed for up to 9 different substrates.

2.6. Data analysis

Statistical analysis was performed by one-way analysis of variance (ANOVA) and post-hoc Turkey–Kramer multiple comparison test. P values less than 0.05 were considered statistically significant. All data are presented as mean ± standard deviation.

3. Results and discussion

3.1. Key characteristics of the starPEG–heparin scaffolds

StarPEG–heparin hydrogel scaffolds differing in the molar ratio of starPEG to heparin (γ) were formed via crosslinking of amino end-functionalized starPEG with EDC/s-NHS-activated carboxylic acid groups of heparin. As shown in Table 1, by increasing the molar ratio of starPEG to heparin from 1.5 to 6 in the initial reaction mixture, stiffer and less hydrated gels could be produced. This finding is related to the increased number of covalent crosslinks and therefore results in the formation of a denser scaffold, which was theoretically predicted by evaluation of the pore size (determined according to the rubber-elasticity theory as described in [33]) (see Table 1). For a more detailed discussion of the network properties the reader is referred to [33].

Independent of the different mechanical properties the networks contained large quantities of ~8 μg heparin per μl gel [33] which remained approximately constant for scaffolds with different molar ratios of starPEG to heparin ($p > 0.05$). To control the cell adhesive characteristics of the hydrogels, EDC/s-NHS activated carboxylic acid groups of the heparin were modified with the integrin-binding cyclic RGDYK peptides (RGD-peptides, Scheme 1) via the amino group of the lysine. Due to the constant concentration of heparin in the mechanically different hydrogels, similar amounts of RGD-peptides (~0.2 μg/μl gel; $p > 0.05$) were immobilized to the different gel types (Table 1) as previously demonstrated by [33]. Consequently, since subsequent biofunctionalization is based on interaction with heparin, structural and mechanical characteristics can be adapted independently on the biofunctionality of the scaffolds.

3.2. Biomodification with FGF-2 and VEGF

3.2.1. FGF-2 and VEGF immobilization

The starPEG–heparin hydrogels closely mimic the characteristics of the ECM by containing large quantities of heparin which bind and stabilize numerous GFs (Scheme 1). To evaluate the potential of our "heparin rich system" the binding of FGF-2 and VEGF, two cytokines that are crucial for the process of angiogenesis, was analyzed. By cLSM studies (Fig. 1, for images see Supplementary data Fig S1), it was demonstrated that for all gel types, both fluorescently-labeled FGF-2 and VEGF (Fig. 1, data shown for the gels with the lowest [left] and the highest [right] crosslinking degree $\gamma = 1.5$ and 6) were able to diffuse into the networks. A homogeneous fluorescence intensity of TAMRA-FGF-2 (Fig. 1, top) within the hydrogel could be observed immediately (~1 min) after applying the protein. In contrast, for TAMRA-VEGF (Fig. 1, bottom) a complete penetration could be observed only after 30 min ~72% for 0.02 h and 89% for 0.5 h; $p < 0.05$ when comparing the different time points for both types of gel (low and high crosslinking degree $\gamma = 1.5$ and 6). This fact could be explained by the larger diameter of VEGF (~6 nm; 38.2 kDa) [40] compared to that of FGF-2 (~3 nm; 17.2 kDa) [41] which might result in a slower diffusion of this cytokine through the gel pores. Neither proteins showed an increase in the relative fluorescence intensity inside both gel networks (after 24 h–60% for FGF-2 and ~90% for VEGF; $p > 0.05$ for gels of low and high crosslinking degree, $\gamma = 1.5$ and 6) and no corresponding decrease in the supernatants (after 24 h–40% for FGF-2 and ~10% for VEGF; $p > 0.05$ for gels of low and high crosslinking degree, $\gamma = 1.5$ and 6) over the course of the experiment. The lower fluorescence intensity of TAMRA-FGF-2 in the hydrogel might result from an increased tendency of this protein to attach to non-specific surfaces not originating from the starPEG–heparin networks or from a decreased heparin binding affinity due to interferences of the attached label with the particular FGF-2 molecular structure [42].

Table 1
Key characteristics of the different starPEG–heparin hydrogel types.

starPEG/heparin ratio [mol/mol]	Heparin content [μg/μl]	RGD content [μg/μl]	Volume swelling [–]	Storage modulus [kPa]	Pore size [nm]
1.5	8.0	0.23	53	0.99	16
3	7.8	0.23	30	2.57	11.7
6	7.4	0.21	22	14.8	6.5

After penetration, both proteins showed a homogenous distribution throughout the entire scaffold (Fig S1, Supplementary data). These findings demonstrate that there were no significant structural heterogeneities in the network and that the mesh sizes of the different hydrogel types did not prevent penetration of the rather small FGF-2 and VEGF molecules. In contrast to that, proteins with dimensions larger than the pore sizes of the gels could be excluded efficiently as shown by [33]. This offers the advantage that, besides the stabilizing effect that heparin exerts on FGF-2 and VEGF and the low tendency of PEG to allow for unspecific protein adsorption, the penetration of some proteases known to degrade FGF-2 or VEGF such as neprilysin (~86 kDa, degradation of FGF-2) [43], matrix metalloproteinase 3 (~54 kDa, degradation of VEGF) [19] or human plasmin 1 (~91 kDa, degradation of FGF-2 and VEGF) [18,44] is prevented by the particular gel structure. In summary, our matrices could act as supportive carriers maintaining the biological activity of the bound cytokines.

Quantitative protein binding studies were performed using ELISA (Fig. 2A), amino acid analysis via HPLC, and radiolabeling studies (Fig S2, Supplementary data). While quantitative differences determined with the three methods might be due to experimental conditions as described by [42], these techniques were applied because all of them delivered the same qualitative results. First, to analyze whether the starPEG–heparin hydrogels could be used as efficient FGF-2 and VEGF storage system, the capacity of the hydrogels to take up various amounts of the GFs was investigated for the gel with the intermediate crosslinking degree, $\gamma = 3$ (Fig. 2A right, Fig. S2, Supplementary data). With any approach, the immobilized quantities at a defined concentration were found to be similar for both proteins. Moreover, a linear correlation between the concentration of the incubation solution and the amount of immobilized FGF-2 or VEGF within the gel could be found. This indicates that no saturation of binding was reached within the concentration range monitored. Due to the high content of heparin in the networks, after incubation with 50 μg/ml protein the molar ratio of heparin to GF was still 26:1 for FGF-2 and 62:1 for VEGF, respectively. As demonstrated for FGF-2 [45], additionally each heparin molecule is able to interact with several GF molecules. Consequently, a saturation of binding will occur only at concentrations much higher than used here, indicating that FGF-2 or VEGF immobilization can be tuned over a broad range.

To compare the FGF-2 or VEGF uptake among the different gel types, a protein concentration of 1 μg/ml was used. Via ELISA (Fig. 2A left), amino acid analysis via HPLC and radiolabeling studies (Fig. S2, Supplementary data), it could be shown that similar quantities of FGF-2 or VEGF were immobilized for each scaffold independently on the gel type (for gels with molar ratios starPEG to heparin of $\gamma = 1.5$; 3 or 6–353 ng FGF-2 and ~349 ng VEGF; $p > 0.05$). This confirms once again that the network accessibility for the proteins is not affected by differences in the network structure (pore size, hydration etc.) and that FGF-2 and VEGF binding correlates only with the constant heparin concentration of the different scaffolds. This heparin binding specificity

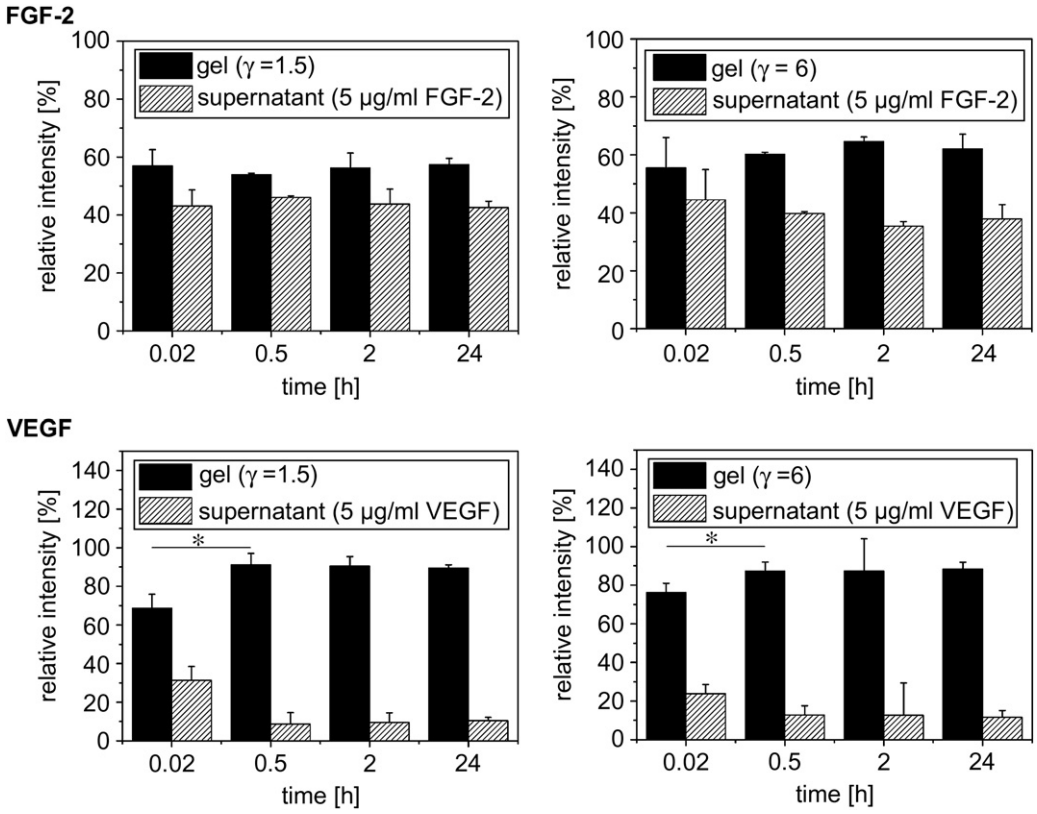

Fig. 1. Average fluorescence intensity of TAMRA-labeled FGF-2 (top) or VEGF (bottom) in the gel with the lowest crosslinking degree $\gamma = 1.5$ (left) or with the highest crosslinking degree $\gamma = 6$ (right) and in the corresponding supernatant at different time point. Measurements were performed using confocal laser scanning microscopy. All data are presented as average over three Z-lines from at least two different gel samples ± root mean square deviation. * indicates statistically significant differences ($p < 0.05$; ANOVA).

could be further validated by the fact that a 100-fold excess of heparin (w/w) in the loading solution almost completely inhibited FGF-2 and VEGF binding to the networks (data not shown). Taken together, the starPEG–heparin hydrogels might be used as highly potent FGF-2 or VEGF storage systems that can present large quantities of the GF independently on the particular structural and mechanical properties of the different scaffolds and could further on maintain the bioactivity of the loaded factors even in presence of proteases.

3.2.2. FGF-2 and VEGF release

Since most biomedical applications require systems that are not only capable of storing large quantities of cellular effectors these biomaterials should also be able to deliver the cytokine to potential target sites. Therefore, after analyzing the FGF-2 and VEGF immobilization to starPEG–heparin hydrogels, experiments on the release of these proteins were performed via ELISA (Fig. 2B) and qualitatively confirmed by radiolabeling studies (data not shown).

First, given the finding that the starPEG–heparin networks could be used as an efficient FGF-2 and VEGF carrier system within a huge range of protein concentrations, the ability of the hydrogels to release various amounts of the GF was investigated by ELISA for FGF-2 (0.5, 1 and 5 µg/ml) or VEGF (1, 5 and 10 µg/ml) immobilized to the gel with the intermediate crosslinking degree, $\gamma = 3$. Fig. 2B (left) illustrates the cumulative release of the protein measured for four days. Both proteins showed an initial burst release within the first 24 h. Such burst characteristics are often attributed to surface effects [46] and could be caused by an FGF-2 or VEGF fraction entrapped in the meshwork but not bound specifically to heparin. However, after 24 h, the release continued slowly over the course of the entire time period that was investigated, indicating the potential of the material for applications with a need for long-term release profiles of GFs. While both proteins showed a similar release profile for a given concentration, the overall release of FGF-2 was higher than for VEGF (e.g. for 5 µg/ml protein after four days ~16 ng FGF-2 and ~9 ng VEGF released; $p < 0.05$). Since the heparin binding affinity of FGF-2 (Kd = 23 nM) is higher than that of VEGF (Kd = 165 nM) [47] an explanation for this finding might be that the larger molecule VEGF diffuses out of the gel matrix more slowly than the smaller FGF-2. Moreover, similar to the protein binding studies, a linear correlation between the amount of bound FGF-2 or VEGF within the gel, which directly depends on the concentration used for immobilization, and the protein quantities being released was observed. Given this finding, the release characteristics can be adjusted by the initial amount of protein loaded which in turn can be tuned over a wide range of concentrations. Further work is now focusing on the modulation of the release characteristics additionally via selective desulfation of the heparin [17,48,49].

To analyze whether the FGF-2 or VEGF sequestering on the meshsize of the particular substrate, in the next step, the cytokine release characteristics were determined for the different gel types (molar ratios starPEG to heparin of $\gamma = 1.5$, 3, and 6) over the course of four days. For these experiments, a protein concentration of 1 µg/ml was used and results were investigated via both ELISA (Fig. 2B) and radiolabeling studies (data not shown). Via both methods, similar kinetics showing an initial burst followed by a slow release over time as well as comparable sequestered quantities of FGF-2 or VEGF were found for each scaffold independently on the gel type (for gels with molar ratios starPEG to heparin of $\gamma = 1.5$, 3, and 6 after four days ~3 ng FGF-2 and ~1.5 ng VEGF released; $p > 0.05$). This result demonstrates once again that the

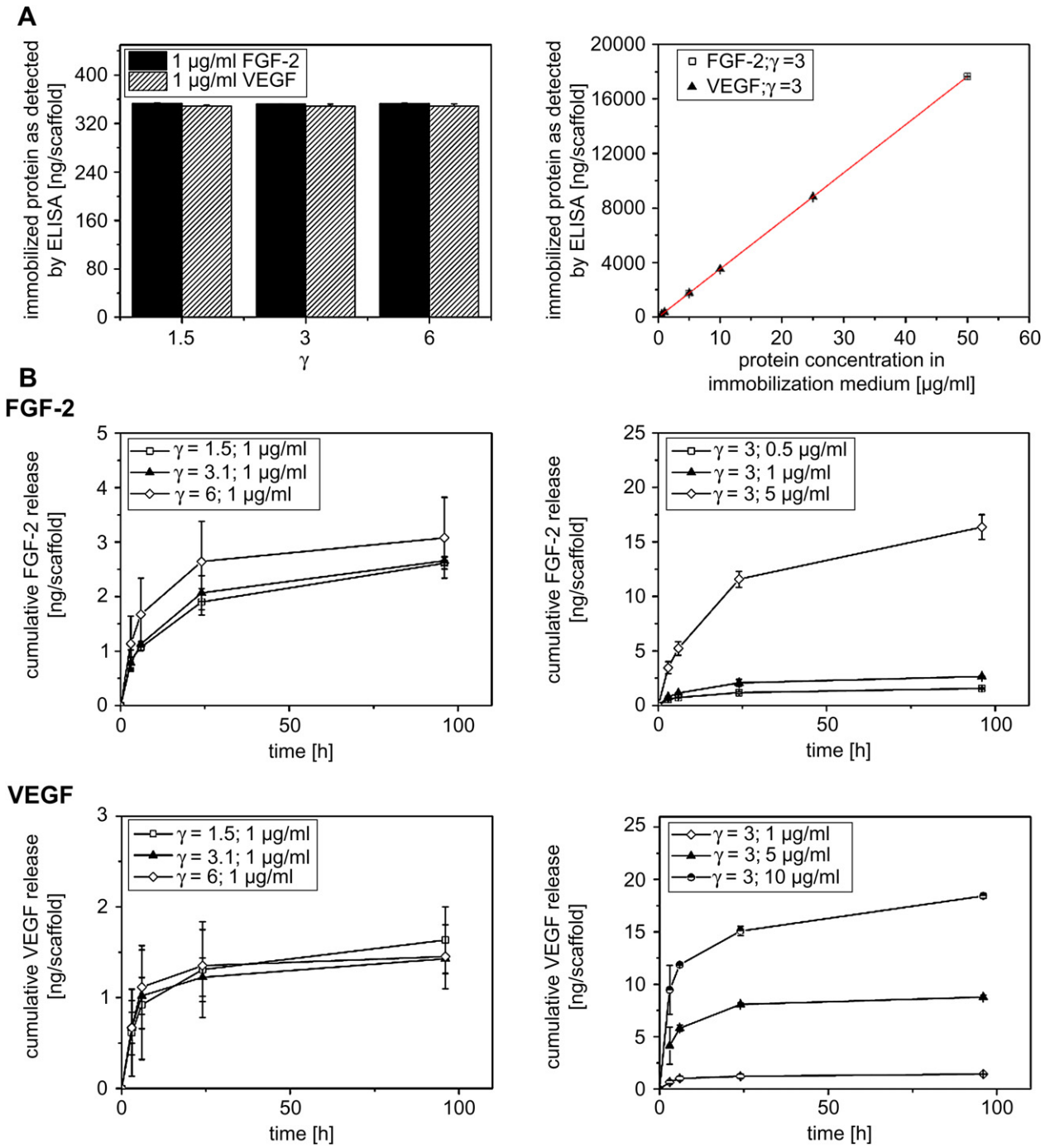

Fig. 2. FGF-2 and VEGF uptake (A) and release (B) experiments for different gel types (left) or protein concentrations (right) quantified via ELISA. 2A (left): amount of electrostatically bound FGF-2 or VEGF per scaffold for the different gel types $\gamma = 1.5$; 3 or 6 (low, intermediate and high crosslinking degree, $p > 0.05$; ANOVA). 2A (right): uptake of FGF-2 or VEGF in dependence on the protein concentration in the immobilization medium; linear regression, R^2 (FGF-2) = 0.99999; R^2 (VEGF) = 0.99999. 2B (left): cumulative amount of electrostatically bound FGF-2 (top) or VEGF (bottom) released by the different gel matrices $\gamma = 1.5$; 3 or 6 (low, intermediate and high crosslinking degree, $p > 0.05$; ANOVA). 2B (left): cumulative release of FGF-2 (top) or VEGF (bottom) in dependence on the protein concentration used for immobilization. All data are presented as mean ± root mean square deviation from $n = 3$.

release of the two proteins is independent on the network structure and that the sequestered quantities seem to depend only on the constant heparin concentration of the different scaffolds.

Conclusively, the results show that the starPEG–heparin hydrogels can be applied as efficient FGF-2 and VEGF storage and delivery systems with well adjustable release characteristics that can be for the first time- decoupled from the structural properties of the scaffolds.

3.2.3. HUVECs response to different types of biomodified starPEG–heparin networks

It has long been known that the process of angiogenesis is tightly controlled by both molecular cues and the physicochemical structure of the surrounding matrix [5]. Consequently, to gain insight into the complex mechanism of its regulation there is a need for in vitro model systems that allow for an independent investigation of both parameters.

To clearly investigate the influence of the different material parameters, endothelial cells were cultured under serum-free conditions on top of hydrogels that differ in terms of their physicochemical characteristics [gels with low, intermediate and high crosslinking degree and therefore low, intermediate and high stiffness and meshsize, respectively ($\gamma = 1.5$, 3 and 6)] along with varying degrees of biofunctionality (pure gels or scaffolds modified with either FGF-2, VEGF or RGD alone as well as a combination of the particular GF and the adhesion ligand). As illustrated previously, the amount of introduced biomolecules was constant among the different gel types (see Table 1 and Fig. 2A). Surfaces consisting of immobilized fibronectin with or without 1 ng/ml FGF-2 or VEGF supplemented to the culture medium were used as controls. This particular cytokine concentration was chosen since it corresponds to the FGF-2 concentration included in common serum-containing medium and relates to the amount of FGF-2 or VEGF that is released by the starPEG–heparin hydrogels within the first hours. For every culture substrate, cellular responses in terms of proliferation/survival and cell morphology were analyzed.

To investigate whether starPEG–heparin hydrogels are able to support HUVEC proliferation and survival as well as to monitor the effect of the biomolecular functionalization and the structural properties, MTT (Fig. 3 B, for statistics see Supplementary data) and live/dead assays (Fig. 3A, green/red cells) were performed after three days of culture on the different substrates. Furthermore, the determination of whether a biomaterial has the potential to support the process of angiogenesis, and not only its ability to promote HUVECs growth and proliferation, is critical. During the process of angiogenesis, the cells differentiate to form tubular structures, in which they adapt a more elongated morphology. Consequently, in this study, HUVECs circularity as it was dependent on the biomolecular functionalization and the structural characteristics of the substrate was analyzed after three days of culture (Fig. 3C, for statistics see Supplementary data).

For the starPEG–heparin hydrogels it could be shown that coinciding with an advancing degree of biofunctionalization, also the HUVECs proliferation/survival rate increased. Very low survival with many dead cells in the surrounding medium could be observed on pure gels, while the few cells being still viable showed a round shape. This might be due to the mainly non-adhesive character of the starPEG therefore leading to the detachment of most cells. The very small number of HUVECs that could be found on the gel surface was most likely only weakly attached, so that cells were consequently not able to proliferate. On starPEG–heparin hydrogels modified with FGF-2 or VEGF, only a slightly increased but not significantly higher number of cells survived. This shows that, although the presence of the cytokines being released from the scaffolds is known to support cell proliferation, without any effective initial attachment HUVECs are not able to survive.

By introducing the adhesion peptide RGD into the starPEG–heparin hydrogels, the HUVEC survival rate could be increased significantly. Under these culture conditions, only very few dead cells were found in the medium while the viable HUVECs adapted also a more elongated morphology. The most important parameter for that might be the fact that these substrates were able to mediate effective initial cell adhesion. Therefore, HUVECs could successfully spread on these scaffolds so that a high number of the primarily plated cells survived. Since these results were observed on the RGD modified starPEG–heparin hydrogels even under serum-free culture conditions, these scaffolds do not exhibit any toxic effects on the cells and might therefore be generally well suited to support growth of HUVECs. Addition of FGF-2 or VEGF to RGD modified hydrogels potentiated this effect. Under these conditions, for the first time proliferation could be observed, since a higher cell number than initially applied was determined after three days of culture. Almost no dead cells were present in the cell culture medium and most viable HUVECs demonstrated the typical spindle-shaped morphology. When comparing the results between the two growth factors, cell numbers on substrates treated with RGD/VEGF were slightly lower than those for cells on gels modified with RGD/FGF-2. One explanation could be that more FGF-2 is released when compared to VEGF (see Fig. 2B). However, since gels modified similarly with higher VEGF concentrations (5 μg/ml) and therefore, resulting in larger quantities being released, did not lead to increasing cell numbers (data not shown), the enhanced cell survival in the presence of FGF-2 could be explained by the fact that FGF-2 has been shown to induce proliferation to a higher extent than VEGF [50]. By contrast, when cultured on substrates modified with RGD/VEGF, HUVECs adapted a more elongated shape than in the presence of FGF-2 (significant differences, see Fig. 3C and Supplementary data), indicating that VEGF might have a bigger impact on controlling cell morphology [51]. Taken together, these results show that due to the synergistic effect of efficient cell adhesion and GF signaling, starPEG–heparin hydrogels with both adhesion ligand and growth factor modification are the most potent in stimulating HUVECs growth (FGF-2) and differentiation (VEGF).

For all three fibronectin control surfaces, cell numbers were comparable to that observed on hydrogels modified with RGD. Although cell survival rates were slightly but not significantly higher on FN + FGF-2 compared to FN + VEGF, no significant positive effect on HUVECs survival via the addition of FGF-2 or VEGF to the cell culture medium was found when compared to pure FN. A reason for that might be that the HUVECs consume the supplied GFs quite fast so that already after three days of culture, no advantageous effect of the cytokines on cell survival was detectable anymore. In contrast, the starPEG–heparin hydrogels are able to deliver FGF-2 or VEGF over an extended period of time (see Fig. 2 B), therefore allowing for a constant cellular access to the GFs. This fact makes the starPEG–heparin hydrogels a beneficial system for long-term cell culture. Despite its low impact on cell survival when initially administered to FN, the addition of VEGF led once again to a more elongated cell morphology, indicating that for supporting such cellular behavior a short-term accessibility of VEGF might be sufficient.

In addition to the biomolecular functionalization, mechanical matrix parameters of engineered materials are important to promote a desired cellular response [52]. starPEG–heparin hydrogels allow for a variation of the mechanical characteristics at constant biofunctionalization with adhesion ligands (RGD) and GFs (FGF-2 and VEGF). In consequence, the gel system permits to unravel the impact of bulk characteristics of materials (i.e., stiffness, meshsize, and hydration) on the proliferation and differentiation of HUVECs without altering the presentation of biomolecular cues.

For pure gels and gels modified with FGF-2 or VEGF, where survival due to lacking adhesion ligands was generally hardly possible, a change in the mechanical properties could not improve either HUVECs proliferation/survival nor cell morphology. However, for substrates modified with RGD, RGD/FGF-2 or RGD/VEGF increasing cell numbers were found on the gels with low starPEG to heparin ratio (more soft and loose networks), indicating that such network structures are most beneficial to promote HUVECs proliferation/survival. However, for the same types of hydrogels, results were different in terms of the effect on cell morphology. In the case of networks modified with RGD, RGD/FGF-2 or RGD/VEGF, HUVECs cultured on the intermediately crosslinked gel type $\gamma = 3$ showed a slightly more elongated shape. This finding is in agreement with results of [5], where it was shown that substrate requirements for endothelial cell growth and

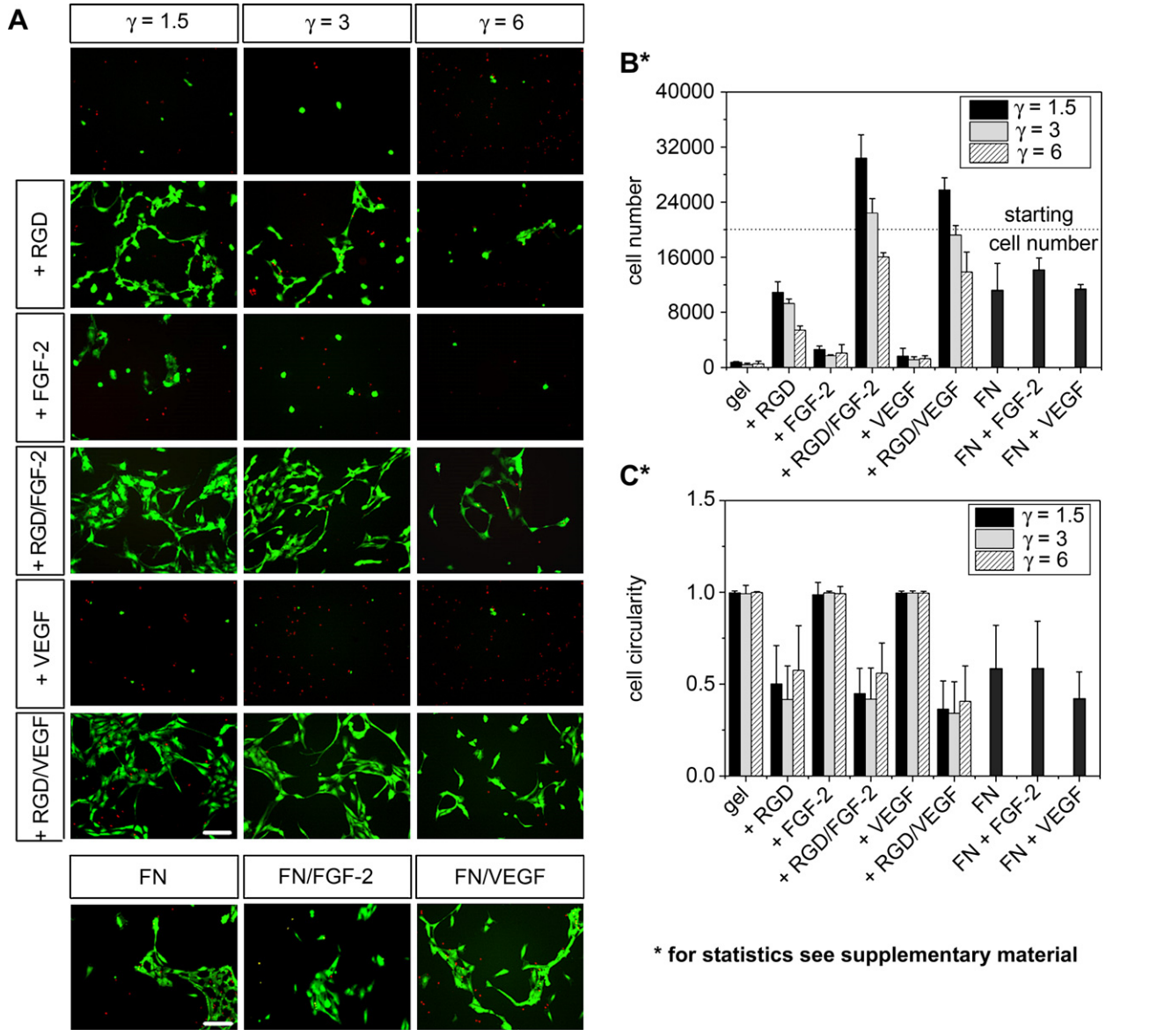

Fig. 3. Interactions of various biomodified hydrogels with HUVECs after 3 days of culture. 3A: representative fluorescence microscopy images after live/dead staining of HUVECs (viable cells = green; dead cells = red) on the different substrates or the corresponding FN controls (scale bar 130 μm). 3B: HUVECs proliferation/survival as accessed via cell numbers on the different networks or the corresponding FN controls quantified by an MTT assay. All data are presented as mean ± root mean square deviation from $n = 3–5$. For statistics see supplementary data. 3C: HUVECs morphology as accessed via cell circularity on the different networks or the corresponding FN controls quantified by the circularity calculation within ImageJ 1.41°. All data are presented as mean ± root mean square deviation from $n \approx 30–200$ cells quantified on up to 9 different substrates. For statistics see supplementary data.

differentiation differ. Under culture conditions that give rise to strong proliferation, thus resulting in confluent monolayer-like growth pattern, cells lose their morphological differences once they form cell-cell contacts [53]. In turn, it has been shown that substrates that were able to turn on endothelial cell differentiation simultaneously switched off cell proliferation [5].

In summary, biomodified starPEG–heparin hydrogels are well-suited substrates for the culture of HUVECs. Moreover, by adjusting the physicochemical structure of the scaffolds independently of the biomolecular functionalization, endothelial cell behavior (e.g. proliferation/survival and morphology) could be tuned. It was found that low starPEG to heparin ratios creating more soft and loose networks in combination with provision of an adhesion ligand and the cytokine FGF-2 showed the most beneficial effects on proliferation/survival. In contrast, hydrogels formed by intermediate starPEG to heparin ratios modified with RGD and VEGF promoted HUVECs differentiation into tube-like structures.

4. Conclusion

StarPEG–heparin hydrogels can be utilized as highly efficient storage and adjustable release systems for various heparin-binding GFs. Based on that, biomolecular and biophysical cues of the modular gel matrix can be varied independently to trigger cellular survival, proliferation and differentiation. Using the resulting options, we were able to demonstrate that HUVECs respond to the provision of FGF-2 and VEGF through engineered gel matrices in ways depending on the adhesiveness and elasticity of the applied materials as well. Systematic variation of multiple biomolecular

signals paralleled by the modulation of viscoelastic characteristics permits the adaptation of the reported gel system to the requirements of an array of tissue engineering applications. The matrix design can be furthermore extended through modification of the building blocks (e.g. the sulfation pattern of heparin) or incorporation of enzymatically cleavable peptide crosslinkers [54]. In sum, starPEG–heparin hydrogels with customized GF delivery profiles afford powerful cell-instructive materials to advance regenerative therapies.

Acknowledgements

We would like to thank Tina Lenk (Leibniz Institute of Polymer Research Dresden) for radiolabeling VEGF, as well as Dr. Mikhail Tsurkan (Leibniz Institute of Polymer Research Dresden) for fluorescence labeling of heparin. U.F. and C.W. were supported by the Deutsche Forschungsgemeinschaft through grants WE 2539-7/1 and FOR/EXC999, and by the Leibniz Association. K.R.L., S.P. and C.W. were supported by the Seventh Framework Programme of the European Union through the Integrated Project ANGIOSCAFF. A.Z. was supported by the Dresden International Graduate School for Biomedicine and Bioengineering.

Appendix. Supplementary data

Supplementary data associated with this article can be found in the online version, at doi:10.1016/j.biomaterials.2010.07.021.

Appendix

Figures with essential colour discrimination. The Scheme 1, Figs. 2 and 3 of this article are difficult to interpret in black and white. The full colour images can be found in the online version, at doi:10.1016/j.biomaterials.2010.07.021.

References

[1] Carmeliet P. Angiogenesis in life, disease and medicine. Nature 2005;438 (7070):932–6.
[2] Patel ZS, Mikos AG. Angiogenesis with biomaterial-based drug- and cell-delivery systems. J Biomater Sci Polym Ed 2004;15(6):701–26.
[3] Chan G, Mooney DJ. New materials for tissue engineering: towards greater control over the biological response. Trends Biotechnol 2008;26:382–92.
[4] Lutolf MP, Hubbell JA. Synthetic biomaterials as instructive extracellular microenvironments for morphogenesis in tissue engineering. Nat Biotechnol 2005;23(1):47–55.
[5] Ingber DE, Folkman J. Mechanochemical switching between growth and differentiation during fibroblast growth factor-stimulated angiogenesis in vitro: role of extracellular matrix. J Cell Biol 1989;109:317–30.
[6] Liu WF, Chen CS. Engineering biomaterials to control cell function. Mater Today 2005;8(12):28–35.
[7] Fischbach C, Mooney DJ. Polymeric systems for bioinspired delivery of angiogenic molecules. Adv Polym Sci 2006;203:191–221.
[8] Taipale J, Keski-Oja J. Growth factors in the extracellular matrix. FASEB J 1997;11(1):51–9.
[9] Presta M, Dell'Era P, Mitola S, Moroni E, Ronca R, Rusnati M. Fibroblast growth factor/fibroblast growth factor receptor system in angiogenesis. Cytokine Growth Factor Rev 2005;16:159–78.
[10] Hoeben A, Landuyt B, Highley MS, Wildiers H, van Oosterom AT, De Bruijn EA. Vascular endothelial growth factor and angiogenesis. Pharmacol Rev 2004;56:549–80.
[11] Pepper MS, Ferrara N, Orci L, Montesano R. Potent synergism between vascular endothelial growth factor and basic fibroblast growth factor in the induction of angiogenesis in vitro. Biochem Biophys Res Commun 1992;189:824–31.
[12] Ferrara N, Alitalo K. Clinical applications of angiogenic growth factors and their inhibitors. Nat Med 1999;5:1359–64.
[13] Tessmar JK, Göpferich AM. Matrices and scaffolds for protein delivery in tissue engineering. Adv Drug Deliv Rev 2007;59:274–91.
[14] Yayon A, Klagsbrun M, Esko J, Leder P, Ornitz D. Cell surface, heparin-like molecules are required for binding of basic fibroblast growth factor to its high affinity receptor. Cell 1991;64:841–8.
[15] Gitay-Goren H, Soker S, Vlodavsky I, Neufeld G. The binding of vascular endothelial growth factor to its receptors is dependent on cell surface-associated heparin-like molecules. Biol Chem 1992;267(9):6093–8.
[16] Faham S, Hileman RE, Fromm JR, Linhardt RJ, Ree DC. Heparin structure and interactions with basic fibroblast growth factor. Science 1996;271 (5252):1116–20.
[17] Ono K, Hattori H, Takeshita S, Kurita A, Ishihara M. Structural features in heparin that interact with VEGF165 and modulate its biological activity. Glycobiology 1999;9(7):705–11.
[18] Saksela O, Moscatelli D, Sommer A, Rifkin DB. Endothelial cell-derived heparan sulfate binds basic fibroblast growth factor and protects it from proteolytic degradation. J Cell Biol 1988;107:743–51.
[19] Lee S, Jilani SM, Nikolova GV, Carpizo D, Iruela-Arispe ML. Processing of VEGF-A by matrix metalloproteinases regulates bioavailability and vascular patterning in tumors. J Cell Biol 2005;169(4):681–91.
[20] Roghani M, Mansukhani A, Dellera P, Bellosta P, Basilico C, Rifkin DB, et al. Heparin increases the affinity of basic fibroblast growth factor for its receptor but is not required for binding. J Biol Chem 1994;269(6):3976–84.
[21] Wissink MJ, Beernink R, Poot AA, Engbers GH, Beugeling T, van Aken WG, et al. Improved endothelialization of vascular grafts by local release of growth factor from heparinized collagen matrices. J Control Release 2000;64(1-3):103–14.
[22] Sakiyama-Elbert SE, Hubbell JA. Development of fibrin derivatives for controlled release of heparin-binding growth factors. J Control Release 2000;65(3):389–402.
[23] Tanihara M, Suzuki Y, Yamamoto E, Noguchi A, Mizushima Y. Sustained release of basic fibroblast growth factor and angiogenesis in a novel covalently crosslinked gel of heparin and alginate. J Biomed Mater Res 2001;56 (2):216–21.
[24] Edelman ER, Mathiowitz E, Langer R, Klagsbrun M. Controlled and modulated release of basic fibroblast growth factor. Biomaterials 1991;12 (7):619–26.
[25] Joung YK, Bae JW, Park KD. Controlled release of heparin-binding growth factors using heparin-containing particulate systems for tissue regeneration. Expert Opin. Drug Deliv 2008;5(11):1173–84.
[26] Jia X, Kiick KL. Hybrid multicomponent hydrogels for tissue engineering. Macromol Biosci 2009;9(2):140–56.
[27] Seal BL, Panitch A. Physical polymer matrices based on affinity interactions between peptides and polysaccharides. Biomacromolecules 2003;4 (6):1572–82.
[28] Benoit DS, Anseth KS. Heparin functionalized PEG gels that modulate protein adsorption for hMSC adhesion and differentiation. Acta Biomater 2005;1 (4):461–70.
[29] Cai S, Liu Y, Zheng Shu X, Prestwich GD. Injectable glycosaminoglycan hydrogels for controlled release of human basic fibroblast growth factor. Biomaterials 2005;26(30):6054–67.
[30] Tae G, Scatena M, Stayton PS, Hoffman AS. PEG-crosslinked heparin is an affinity hydrogel for sustained release of vascular endothelial growth factor. J Biomater Sci Polym Ed 2006;17(1–2):187–97.
[31] Nie T, Akins Jr RE, Kiick KL. Production of heparin-containing hydrogels for modulating cell responses. Acta Biomater 2009;5:865–75.
[32] Tessmar JK, Gopferich AM. Customized PEG-derived copolymers for tissue-engineering applications. Macromol Biosci 2007;7(1):23–39.
[33] Freudenberg U, Hermann A, Welzel PB, Stirl K, Schwarz SC, Grimmer M, et al. A starPEG–heparin hydrogel platform to aid cell replacement therapies for neurodegenerative diseases. Biomaterials 2009;30:5049–60.
[34] Pompe T, Zschoche S, Herold N, Salchert K, Gouzy MF, Sperling C, et al. Maleic anhydride copolymers - a versatile platform for molecular biosurface engineering. Biomacromolecules 2003;4:1072–9.
[35] Salchert K, Pompe T, Sperling C, Werner C. Quantitative analysis of immobilized proteins and protein mixtures by amino acid analysis. J Chromatogr A 2003;1005:113–22.
[36] Weis JR, Sun B, Rodgers GM. Improved method of human umbilical arterial endothelial cell culture. Thromb Res 1991;61:171–3.
[37] Brew SA, Ingram KC. Purification of human plasma fibronectin. J Tissue Cult Methods 1994;16:197–9.
[38] Jones KH, Senft JA. An improved method to determine cell viability by simultaneous staining with fluorescein diacetate – propidium iodide. J Histochem Cytochem 1985;33:77–9.
[39] Supino R. MTT assays. Methods Mol Biol 1995;43:137–49.
[40] Muller YA, Li B, Christinger HW, Wells JA, Cunningham BC, de Vos AM. Vascular endothelial growth factor: crystal structure and functional mapping of the kinase domain receptor binding site. Proc Natl Acad Sci USA 1997;94 (14):7192–7.
[41] Eriksson AE, Cousens LS, Weaver LH, Matthews BW. Three-dimensional structure of human basic fibroblast growth factor. Proc Natl Acad Sci USA 1991;88(8):3441–5.
[42] Zieris A, Prokoph S, Welzel PB, Grimmer M, Levental KR, Panyanuwat W, et al. Analytical approaches to uptake and release of hydrogel-associated FGF-2. J Mater Sci Mater Med 2010;21(3):914–23.
[43] Goodman Jr OB, Febbraio M, Simantov R, Zheng R, Shen R, Silverstein RL, et al. Neprilysin inhibits angiogenesis via proteolysis of fibroblast growth factor-2. J Biol Chem 2006;281(44):33597–605.
[44] Keyt BA, Berleau LT, Nguyen HV, Chen H, Heinsohn H, Vandlen R, et al. The carboxyl-terminal domain (111-165) of vascular endothelial growth factor is critical for its mitogenic potency. J Biol Chem 1996;271(13):7788–95.

[45] Arakawa T, Wen J, Philo JS. Stoichiometry of heparin binding to basic fibroblast growth factor. Arch Biochem Biophys 1994;308(1):267–73.
[46] Huang X, Brazel CS. On the importance and mechanisms of burst release in matrix-controlled drug delivery systems. J Control Release 2001;73(2–3):121–36.
[47] Ashikari-Hada S, Habuchi H, Kariya Y, Itoh N, Reddi AH, Kimata K. Characterization of growth factor-binding structures in heparin/heparan sulfate using an octasaccharide library. J Biol Chem 2004;279(13):12346–54.
[48] Casu B, Naggi A, Torri G. Chemical derivatization as a strategy to study structure-activity relationships of glycosaminoglycans. Semin Thromb Hemost 2002;28(4):335–42.
[49] Freeman I, Kedem A, Cohen S. The effect of sulfation of alginate hydrogels on the specific binding and controlled release of heparin-binding proteins. Biomaterials 2008;29(22):3260–8.
[50] Yoshida A, Anand-Apte B, Zetter BR. Differential endothelial migration and proliferation to basic fibroblast growth factor and vascular endothelial growth factor. Growth Factors 1996;13(1–2):57–64.
[51] Goto F, Goto K, Weindel K, Folkman J. Synergistic effects of vascular endothelial growth factor and basic fibroblast growth factor on the proliferation and cord formation of bovine capillary endothelial cells within collagen gels. Lab Invest 1993;69(5):508–17.
[52] Discher DE, Mooney DJ, Zandstra PW. Growth factors, matrices, and forces combine and control stem cells. Science 2009;324:1673–7.
[53] Yeung T, Georges PC, Flanagan LA, Marg B, Ortiz M, Funaki M, et al. Effects of substrate stiffness on cell morphology, cytoskeletal structure, and adhesion. Cell Motil Cytoskeleton 2005;60:24–34.
[54] Tsurkan MV, Levental KR, Freudenberg U, Werner C. Enzymatically degradable heparin–polyethylene glycol gels with controlled mechanical properties. Chem Commun 2010;46:1141–3.